Simulating and Validating Facial Expressions using an Anatomically Accurate Biomechanical Model Derived from MRI Data

Towards Fast and Realistic Generation of Animated Characters

Tim Wu, Peter Hunter and Kumar Mithraratne
Auckland Bioengineering Institute, The University of Auckland, Auckland, New Zealand

Keywords: Facial Animation, Anatomical Facial Geometry, Finite Deformation Elasticity, Muscle-driven Model.

Abstract: A detailed high-order (cubic-Hermite) finite element model of the human head was constructed from anatomical data segmented from MR images. The model includes a superficial soft-tissue mesh (skin, subcutaneous layer and superficial musculo-aponeurotic system), 20 muscles of facial expressions and several deep structures. Based on the theory of finite deformation elasticity together with large deformation contact constraints, quasi-static facial expressions were generated by activating transversely isotropic muscles that were accurately depicted by their respective anatomical geometries. Material (muscle-fat) heterogeneity was also introduced to capture the realistic formation of skin folds. Using the described approach, four facial expressions were simulated and compared with the surface data obtained from a 3D structured-light scanner. Predicted expressions showed good agreement with the experimental data.

1 INTRODUCTION

Generating realistic facial expressions have always been a key area of research in the animation industry. Traditional techniques often rely on the geometric models that are driven by motion capture data. As the computational technologies advance, it becomes increasingly viable to use physics-based techniques to predict facial movements based on the contraction of underlying muscles. In comparison to the data-driven approach, a physics-based face model can produce realistic facial gestures while interacting with foreign objects or the environment (Sifakis et al., 2005).

Some previous physics-based models simplified the facial soft tissues as a mass-spring lumped parameter system (Zhang et al., 2006) or as a linear elastic continuum (Gladilin et al., 2004); (Chabanas and Payan, 2000). However, these linear models are inadequate as facial soft tissues often undergo large local rotations and straining, in which nonlinear, finite deformation elasticity theory is more appropriate (Grioli, 1997). Moreover, almost all earlier models had their muscle geometries constructed from 1D line segments or primitive 3D shapes. As a result, the predictive power of these models was limited. More recently, Barbarino et al. (2009) developed a face model based on the data segmented from on MR images. But despite the detailed representation of anatomical parts, their model lacks the active (muscle-driven) mechanics essential for generating facial expressions.

In this study, anatomically accurate 3D muscles driven by phenomenological muscle actuators were used for mechanics simulation. In addition, finite deformation elasticity theory with a nonlinear constitutive relation was employed to fully describe the anticipated large deformation of the soft tissue structures.

2 METHOD

2.1 Anatomical Data

Anatomical data were collected from the MR images of a healthy 26 year-old male volunteer. An auto-segmentation algorithm was used for 1odeling1g the skin surface, while the muscles of facial expression and other deep structures were segmented manually (Figure 1) using the CMGUI 1 odeling package (http://www.cmiss.org/cmgui). Bilateral symmetry (symmetry along the mid-sagittal plane) was assumed, and only the right half of the head was

Wu T., Hunter P. and Mithraratne K..
Simulating and Validating Facial Expressions using an Anatomically Accurate Biomechanical Model Derived from MRI Data - Towards Fast and Realistic Generation of Animated Characters.
DOI: 10.5220/0004293502670272
In *Proceedings of the International Conference on Computer Graphics Theory and Applications and International Conference on Information Visualization Theory and Applications* (GRAPP-2013), pages 267-272
ISBN: 978-989-8565-46-4

considered. For the purpose of visualisation, the left half of the head was created by mirroring the geometry of all structures in the mid-sagittal plane.

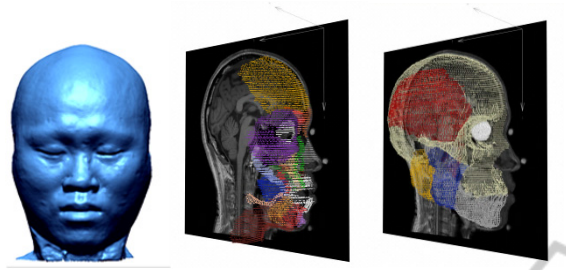

Figure 1: 3D data cloud of the segmented skin surface (left), muscles of facial expression (centre) and deep structures (right).

2.2 Finite Element Model

A complex network of muscles is found inside the superficial fascia of the face, where it is tightly connected to the surrounding adipose and connective tissues (Mendelson, 2009). To model this behaviour, a finite element volume (3D) mesh was created for the entire superficial soft tissue mass consisting of skin, subcutaneous layer and the superficial musculo-aponeurotic system (SMAS) (Mitz and Peyronie, 1976). Moreover, finite element meshes of individual muscles, glands and skeletal bones were also generated. Some of the muscles (specifically, the muscles of facial expression) were embedded inside the superficial fascia to account for varying mechanical properties, while deep structures were regarded as separate entities which mechanically interact with the superficial continuum mesh. Figure 2 shows the geometric meshes created by fitting to the segmented data.

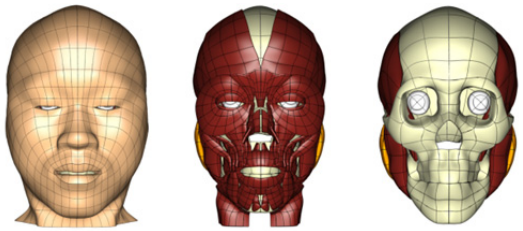

Figure 2: Fitted geometric meshes of the superficial soft tissue continuum (left), muscles of facial expression (centre) and deep structures (right).

Since the muscles of facial expression are embedded inside the deformable superficial continuum mesh, these muscles do not introduce additional degrees of freedom to the problem. In total, the continuum model is composed of 229 volume elements and 493 nodes interpolated using cubic-Hermite basis functions (Bradley et al., 1997). Cubic-Hermite interpolations were used as they provide C^1-continuous displacement field therefore satisfying moment balance during large bending and torsional deformations (Desai and Kundu 2001).

2.2.1 Correction for Gravity

The MRI data were acquired with the subject lying in supine position due to limited space inside the MRI scanner. This is different to an animation setting, where the head is usually in an upright pose. As a consequence, the gravity induced deformations were different. Since gravity is neglected in this study, the reference state for the mechanical analysis is defined to be at the upright position. The upright configuration for the finite element model was determined by fitting the superficial continuum mesh to the neutral expression (all muscles relaxed) structured-light surface data acquired in the upright position. The underlying muscles were also customised to reflect the new configuration. The fitting and customisation procedures employed in this paper are documented in detail in (Fernandez et al., 2004).

2.3 Finite Deformation Elasticity and Contact Modelling

The governing equation for a 3D continuum under static equilibrium is given as

$$\frac{\partial \sigma_{ij}}{\partial x_i} + b_j = 0 \qquad (1)$$

where σ_{ij} are the components of the Cauchy stress tensor, x_i are spatial coordinates, and b_j are the components of the body force vector. In this study body forces were neglected and hence removed from the governing equation. The facial soft tissues were assumed to be hyperelastic and were approximated using the two-parameter Mooney-Rivlin constitutive model.

$$w = c_1(\bar{I}_1 - 3) + c_2(\bar{I}_2 - 3) \qquad (2)$$

Here, w is the strain energy density function, c_1 and c_2 are the material parameters, $\bar{I}_1$ and $\bar{I}_2$ are the isochoric strain invariants (Flory, 1961). Furthermore, the material was assumed to be incompressible in which the incompressibility constraint is enforced using the method of Lagrange multipliers.

To avoid penetrations between the continuum

mesh and the deep structures, surface to surface contact constraints were imposed using the penalty method. In addition, certain nodes of the continuum mesh were precisely positioned to represent attachment locations of the ligaments and muscle origins where displacement boundary constraints were placed to mimic these fixation sites.

2.3.1 Material Heterogeneity

Material heterogeneity of the facial soft-tissues arises from the integrated structures of different tissue types such as muscles, fat (adipose tissue), aponeurosis and other connective tissues. In addition, local variations within each tissue type also contribute to heterogeneous mechanical response. Since it is impractical to model all structural variations, only the heterogeneity caused by the elastic difference between the muscular and adipose tissues were modelled.

The distribution of these two tissues was represented as a percentage of the volume occupied by each constituent. Accordingly, a finite element field can be used to describe the variation of these percentages across the computational domain. The material parameters assigned for the 100% muscular and 100% adipose tissues are given in table 1, whereas the regions with mixed percentage of materials were linearly interpolated based on the relative fraction.

Table 1: Mooney-Rivlin material parameters.

Fat (Tran et al., 2007)	Muscle (Nazari et al., 2010)
$c_1 = 0.42\text{kPa}$	$c_1 = 2.500\text{kPa}$
$c_2 = 0.00\text{kPa}$	$c_2 = 1.175\text{Pa}$

2.3.2 Muscle Mechanics

The mechanical contribution of the muscle structure depends primarily on the response of its constituents, namely, the muscle fibres and surrounding matrix. Muscle fibres are responsible for the active contraction of the muscle structure. It is well-known that the active tension produced by a muscle fibre is a function of its stretch ($\lambda = l/l_0$), where l_0 and l are the reference and current fibre lengths respectively. For skeletal muscles, active tension curve has a maximum at the experimentally determined optimal fibre stretch λ_{ofl}. In addition, it is also observed that muscle fibres developed passive restorative forces when elongated beyond the optimal fibre stretch (Zajac, 1989). The total stress produced by muscle fibres is given as

$$\sigma_{ij}^{m} = \frac{\lambda\sigma_{max}}{\lambda_{ofl}}\left(af_{act} + f_{pas}\right)\frac{\partial x_i}{\partial v_f}\frac{\partial x_j}{\partial v_f} \qquad (3)$$

where σ_{max} is the maximum active stress developed by the fibre at the optimal stretch, a is the level of activation, f_{act} and f_{pas} are the normalised active and passive fibre tension respectively given by the classical force-stretch relationship (Blemker et al., 2005) and v_f are the components of the fibre axes.

Moreover, the fibres in some muscles are arranged in an oblique angle to the muscle length, such as the buccinator muscle. To describe the locally varying fibre directions, Euler angles were introduced to rotate the fibre axis (Mithraratne et al., 2010). Figure 3 illustrates the fibre arrangement of three of the facial muscles. For the present studies, these information were obtained by consulting anatomical literature. Figure 4 demonstrates the importance of the fibre orientation in obtaining physiologically realistic deformations.

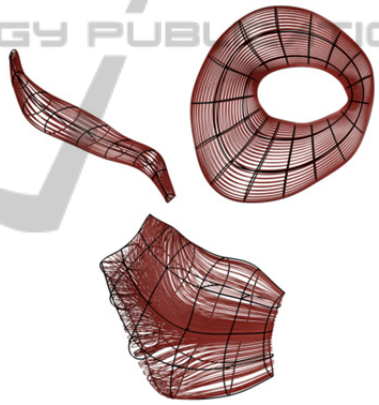

Figure 3: Muscle fibre arrangement of the zygomaticus major muscle (left), orbital belly of the orbicularis oculi muscle (centre) and the buccinator muscle (right).

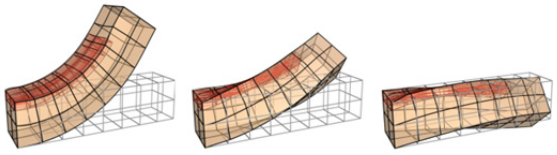

Figure 4: Deformation of a rectangular beam as a result of activation of a muscle slab embedded inside the beam. Showing muscle fibre angles of (from left to right) 0°, 36° and 60° from the longitudinal axis of the beam.

3 SIMULATION RESULTS

Most complex facial expressions can be obtained as

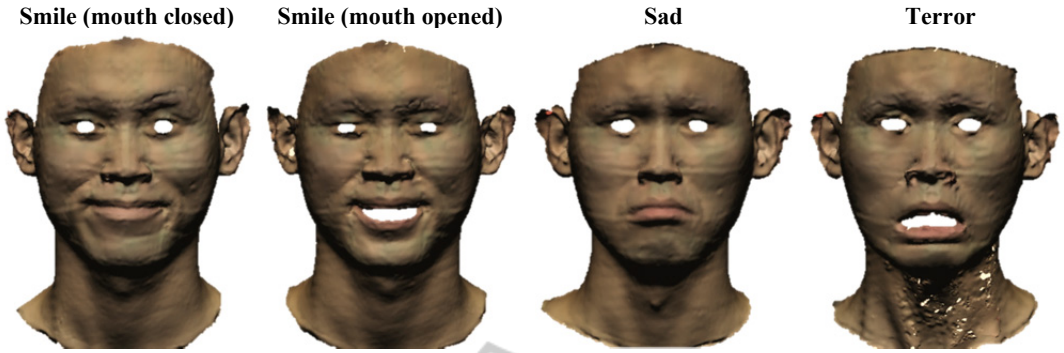

Figure 5: 3-D surface data of four primary facial expressions obtained from structured-light 3D scanner.

a combination of elementary actions produced from single muscles. It is useful to visualise the individual muscle actions before designing an input parameter space (level of activations) for a given facial expression. Therefore, a series of exploratory simulations were conducted by activating one muscles at a time (see figure in the Appendix).

In this section, four well-known facial expressions were generated using the developed model. Figure 5 depicts the surface data cloud obtained from 3D structured light scanner for these expressions. The muscles employed to produce these expressions are listed in Table 2.

Table 2: Muscles employed for the facial expressions simulated.

expression	Activated muscles
Smile (mouth closed)	Buccinator, levator anguli oris, orbicularis oculi (orbital part), risorius, zygomaticus major and zygomaticus minor.
Smile (mouth opened)	Depressor labii inferioris, levator anguli oris, levator labii superioris alaeque nasi, orbicularis oculi (orbital part), zygomaticus major and zygomaticus minor.
Sad	Corrugator, depressor anguli oris, frontalis, mentalis, orbicularis oris, platysma and risorius.
Terror	Depressor anguli oris, depressor labii inferioris, frontalis, mentalis, platysma and risorius.

The simulation results are shown in Figure 6, with each simulation took approximately 2 hours on a standard quad-core computer (2.4GHz). Prediction error was estimated by projecting the structured-light surface data (Figure 5) to the deformed configurations obtained from the model (Figure 6). The RMS errors were 0.88mm, 0.93mm, 1.43mm, 1.40mm for smile with mouth closed, smile with mouth opened, sad and terror expressions respectively. In all simulations, higher errors (>4mm) were observed at the corners of the lips due to more significant displacements. Moreover, in the sad expression, protrusion of the lips was seen in the scanned data which was not captured in the simulations. This is possibly due to the fact that the orbicularis oris and levator muscles were also activated when the subject was asked to perform the expression. It shall also be noted that, in this study, the activation parameters were heuristically assigned from experience; smaller projection errors may be achieved if these parameters (level of activations) were determined by optimising (minimising) against the data error.

4 CONCLUSIONS AND FUTURE WORK

A high-order, heterogeneous finite element model of the head was developed. The deformed state of the model was predicted using physical theory governed by finite deformation elasticity. In addition to material heterogeneity, anisotropic property was also introduced by embedding anatomically accurate 3D muscles with preferential fibre direction. The simulated deformation from the model has shown good match with experimental data where the errors can be further minimised through a more rigorous parameter identification procedure.

This model is a part of the framework that is currently being developed towards a biophysically based computational model for facial expression simulations. With further development, this model will also be useful in the medical sector, such as predicting the muscular functions after plastic and reconstructive operations. While solving these nonlinear mechanics equations are time consuming

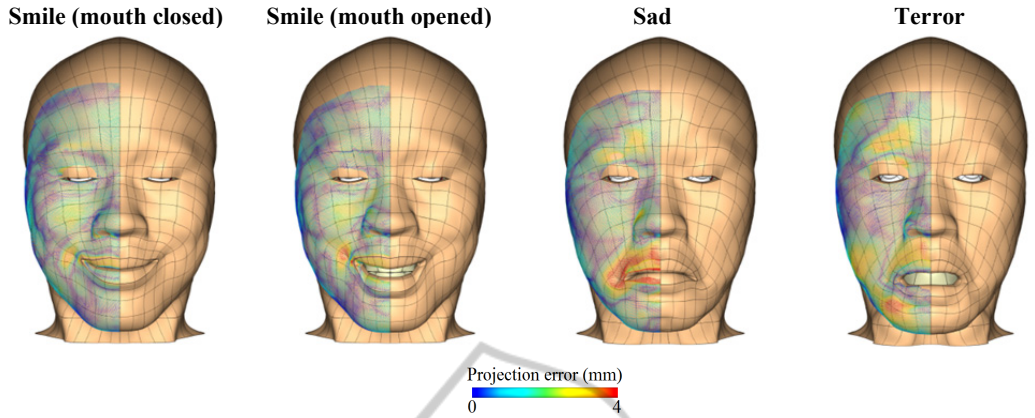

Figure 6: Numerical simulations of four primary facial expressions, showing the projection errors between the simulated deformed configuration and structure-light surface data.

and not practical for interactive applications, they can be useful in generating data sets for fast surrogate-based modelling (Queipo et al., 2005). Work on the surrogate-based modelling technique is already underway. In addition, using appropriate fitting and customisation procedures, the detailed finite element model developed in this study can be readily morphed into another subject, hence reducing the manual intensive effort when creating a population of face models.

ACKNOWLEDGEMENTS

The work presented in this paper was funded by Foundation for Research, Science and Technology of New Zealand under the grant number UOAX0712.

REFERENCES

Barbarino, G. G., Jabareen, M., Trzewik, J., Nkengne, A., Stamatas, G. & Mazza, E., 2009. 'Development and validation of a three-dimensional finite element model of the face', *Journal of Biomechanical Engineering*, vol. 131, no. 4, pp. 041006.

Blemker, S. S., Pinsky, P. M. & Delp, S. L., 2005. 'A 3D model of muscle reveals the causes of nonuniform strains in the biceps brachii', *Journal of Biomechanics*, vol. 38, pp. 657-665.

Bradley, C. P., Pullan, A. J. & Hunter, P. J., 1997. 'Geometric modeling of the human torso using cubic hermite elements', *Annals of Biomedical Engineering*, vol. 25, pp. 96-111.

Chabanas, M. & Payan, Y., 2000. 'A 3D finite element model of the face for simulation in plastic and maxillo-facial surgery', *Lecture Notes in Computer Science*, vol. 1935/2000, pp. 411-496.

Desai, C. S. & Kundu, T., 2001. *Introductory finite element method*, CRC Press, Boca Raton.

Fernandez, J. W., Mithraratne, P., Thrupp, S. F., Tawhai, M. H. & Hunter, P. J., 2004. 'Anatomically based geometric modelling of the musculo-skeletal system and other organs', *Biomechanics and Modeling in Mechanobiology*, vol. 2, no. 3, pp. 139-155.

Flory, P. J., 1961. 'Thermodynamic relations for high elastic materials', *Transactions of the Faraday Society*, vol. 57, pp. 829-838.

Gladilin, E., Zachow, S., Deuflhard, P. & Hege, H. C., 2004. 'Anatomy- and physics-based facial animation for craniofacial surgery simulations', *Medical and Biological Engineering and Computing*, vol. 42, pp. 167-170.

Grioli G., 1997. 'Comparison between finite and linear elasticity', *Applicable Analysis*, vol. 65, no. 1-2, pp. 145-151.

Mendelson, B., 2009. 'Facelift anatomy, SMAS, retaining ligaments and facial spaces', in *Aesthetic plastic surgery*, eds S. J. Aston, D. S. Steinbrech & J. walden, Saunders, Edinburgh.

Mithraratne, K., Hung, A., M.Sagar & Hunter, P. J., 2010. 'An efficient heterogeneous continuum model to simulate active contraction of facial soft tissue structures', in *6th World Congress of Biomechanics (WCB 2010); August 1-6, 2010*, eds C. T. Lim & J. C. H. Goh, Springer, Berlin.

Mitz, V. & Peyronie, M., 1976. 'The superficial musculo-aponeurotic system (SMAS) in the parotid and cheek area', *Plastic and Reconstructive Surgery*, vo. 58, pp. 80-88.

Nazari, M. A., Perrier, P., Chabanas, M. & Payan, Y., 2010. 'Simulation of dynamic orofacial movements using a constitutive law varying with muscle activation'. *Computer Methods in Biomechanics and Biomedical Engineering*, vol. 13, pp. 469-482.

Queipo, N. V., Haftka, R. T., Shyy, W., Goel, T., Vaidyanathan, R. & Tucker, P. K., 2005. 'Surrogate-

based analysis and optimization', *Progress in Aerospace Sciences*, vol. 41, no. 1, pp. 1-28.

Sifakis, E., Neverov, I. & Fedkiw, R., 2005. 'Automatic determination of facial muscle activations from sparse motion capture marker data'. *ACM Transactions on Graphics*, vol. 24, pp. 417-425.

Tran, H. V., Charleux, F., Rachik, M., Ehrlacher, A. & Ho Ba Tho, M. C., 2007. 'In vivo characterization of the mechanical properties of human skin derived from MRI and indentation techniques', *Computer Methods in Biomechanics and Biomedical Engineering*, vol. 10, pp. 401-407.

Zajac, F. E., 1989. 'Muscle and tendon: properties, models, scaling, and application to biomechanics and motor ,control', *Critical Reviews in Biomedical Engineering*, vol. 17, pp. 359-411.

Zhang, Y., Sim, T., Tan, C. L. & Sung, E., 2006. 'Anatomy-based face reconstruction for animation using multi-layer deformation', *Journal of Visual Languages and Computing*, vol. 17, pp. 126-160.

APPENDIX

Figure A: Simulated deformations due to individual muscle actions.